

Task-Aware Meta Learning-based Siamese Neural Network for Classifying Control Flow Obfuscated Malware

Jinting Zhu^{1*}, Julian Jang-Jaccard¹, Amardeep Singh¹, Paul A. Watters² and Seyit Camtepe³

¹Cybersecurity Lab, Massey University, Auckland, NEW ZEALAND.

²Cyberstronomy Pty Ltd, AUSTRALIA.

³Data61, CSIRO, AUSTRALIA.

*Corresponding author(s). E-mail(s): jzhu3@massey.ac.nz;

Abstract

Malware authors apply different techniques of control flow obfuscation to create new malware variants to avoid detection. Existing Siamese Neural Network (SNN) based malware detection methods fail to correctly classify different malware families when such obfuscated malware samples are present in the training dataset resulting in high false-positive rates. To address this issue, we propose a novel Task-Aware Meta Learning-based Siamese Neural Network resilient against the presence of malware variants affected by such control flow obfuscation techniques. Using the average entropy features of each malware family as inputs in addition to the image features, our model generates the parameters for the feature layers to more accurately adjust the feature embedding for different malware families each of which have obfuscated malware variants. In addition, our proposed method can classify malware classes even if there are only one or a few training samples available. Our model utilizes a meta-learning with the extracted features of a pre-trained network (e.g., VGG-16) to avoid the bias typically associated with a model trained with a limited number of training samples. Our proposed approach is highly effective in recognizing unique malware signatures, thus correctly classifying malware samples that belong to the same malware family even in the presence of obfuscated malware variants. Our experimental results, validated with N-way on N-shot learning, show that our model is highly effective in classification accuracy compared to other similar methods.

Keywords: Siamese Neural Network, Meta Learning, Feature Embedding, Embedding Space, Malware Classification, Code Obfuscation, Few-shot Learning

1 Introduction

The malware producers are ever more motivated to create new variants of malware to gain profits from unauthorized information stealth. According to the malware detection agency AV Test¹, there are 100 million new variants of malware generated

from January to October 2020 which translates as roughly three thousand new malware daily.

Especially, we have witnessed the fast growth of mobile-based malware. The NTSC report published in 2020² reported that 27% of organizations globally were impacted by malware

¹<https://www.av-test.org/en/statistics/malware/>

²<https://www.ntsc.org/assets/pdfs/cyber-security-report-2020.pdf>

attacks sent via Android mobile devices. In recent times, we have seen malware producers employ techniques such as obfuscation [2, 5, 6] and repackaging [17, 35, 47], mostly through the change of static features [13, 37, 48] to avoid detection. Realizing the trend in the growth of mobile-based malware attacks, there have been numerous Artificial Intelligence (AI)-based defense techniques proposed [12, 19, 20, 33, 36, 41].

We argue that there are two large issues to be addressed in the existing state-of-the-art of AI-based mobile malware attack defense.

The first issue is the majority of existing research tends to focus on learning from common semantic information of the generic feature of malware families and building feature embeddings [9, 30, 31]. Here the feature embedding represents the features contained in a malware binary sample to provide an important clue as to whether the malware image the feature embedding is created from is malicious or not. If malicious, what type of malware family it belongs to assess and build the right set of response strategies. These existing works often treat the fraction of the code changed by the obfuscation and repackaging as a type of noise [8] thus tend to ignore the effect of the modification. This is in large because the code changed by the obfuscation and repackaging techniques show a similar appearance when malware visualization techniques are applied [1, 26, 28]. Using the common semantic information as data input points to feed into a deep neural network cannot capture unique characteristics of each malware family signature thus they will not be able to accurately classify many variants driven from the same malware family [15, 24, 41, 45], especially if an obfuscation technique is applied.

The second issue with the existing approaches is the demand for large data inputs to find more relevant correlations across the features. They are unable to detect and classify the malware families trained with a limited number of samples (e.g., newly emerging variants of malware) [3].

To address these two important issues, we propose a novel task-aware meta learning-based Siamese Neural Network capable of detecting obfuscated malware variants belonging to the same malware family even if only a small number of training samples are available.

The contributions of our proposed model are following:

- Our proposed model can learn a unique malware signature across malware families using the meta-learning even if obfuscated malware samples exist in each malware family.
- Each CNN branch of our proposed SNN model is equipped with two sub-networks: a task-aware meta learner network and an image network, respectively. The task-aware meta learner network generates task-specific weights using the entropy graphs that capture the unique signatures of different malware families. This weight parameter is combined with the shared weights of two CNNs for the feature layers so that feature embedding at each CNN is accurately adjusted for different malware families.
- Our task-aware meta learner network combines entropy attributes with image-based features for malware detection and classification. The combined features are fed to the pre-trained VGG-16 network. By utilizing the VGG-16 network as a part of the meta-learning process, the weight generator generates the weights that accurately capture the combined features. This can avoid the potential issue of introducing bias in weight generation when the training sample size is limited.
- Our proposed model uses two different types of loss functions that can more accurately compute the similarity scores for the features within the feature embedding of each CNN (i.e., inter-class variance) and across the feature embeddings of two CNNs (i.e., intra-class variance). For the embedding loss to compute the inter-class variance, we add a secondary embedding loss alongside the binary loss to improve the bias that is introduced by a limited size of training samples. For the hybrid loss to compute the intra-class variance, the center loss is added alongside the contractive loss to enable positive pairs and negative pairs to form more distinct clusters across the pairs of images processed by two CNNs.
- Our extensive experiments with N-way on N-shot learning on the Andro-dumpy dataset show that our proposed model is highly effective to recognise the presence of a unique malware signature thus correctly classifying malware

samples that belong to the same malware family despite the presence of obfuscation techniques. Our classification accuracy is at >91% exceeding the performance of similar methods.

We organize the rest of the paper as follows. We examine the related work in Section 2. We provide the preliminary that describes how a control flow obfuscated malware variants are created and addresses the issues as to why the generic SNN approach would not work to detect such obfuscated malware variants in Section 3. We provide the details of our proposed model along with the details of the main components, their roles and responsibilities, and an overview of the algorithm involved in Section 4. In Section 5, we describe the details of the dataset, feature extraction, and the experimental results with analysis. Finally, we provide a conclusion of our work including the limitation of our proposal and future work directions in Section 6.

2 Related work

In this section, we review two lines of research relevant to our study. These include few-shot learning-based malware detection and feature embedding applied for malware detection.

2.1 Few-shot Learning for Malware Detection

One-shot learning is a method to utilize prior knowledge to learn a generic feature with a few image samples. This method has been widely applied in several applications for example in the field of image classification and recognition, speech recognition, using the Siamese Neural Network and Prototypical Network. Sun et al. [38] proposed a static method to analyze the assembly language operation code through the visualization of malicious code. More recently, Hsiao et al. [12] developed an end-to-end framework based on a Siamese Neural Network to detect malware. Moustakidis et al. [25] attempted the transformation of raw data using fuzzy class memberships which then feed into the Siamese Neural Network to defend against the intrusion attack. Although these researches have achieved competitive results utilizing different feature

extraction techniques, they are limited to learning a semantic feature embedding to distribute tasks more effectively. However, the description of the semantic information of raw binary files they used was not clear and it was difficult to see how these were used for feature embedding. It appeared that a model learned for a generic feature from rare categories was unrealistic to capture the common attribute of malicious code. Tang et al. [39] proposed a high-level malware class feature with a meta-learner and evaluated that their proposal was effective at detecting the malware with distinct features. However, this set of works does not consider the distance between the positive pairs and negative pairs therefore the problem with the precise capture of the distance across intra-class variance still exists. Many existing state-of-the-arts proposed by these existing few-shot learning models tend to employ the contrastive loss which we believe does not contribute towards shrinking the intra-class variance. To resolve this issue, the positive and negative pairs must be effectively separated by the hyperplane. Based on this concept, we propose a hybrid loss function with a center loss combined with a constractive function to improve the positive and negative pairs interval as well as the inter-class variance.

2.2 Feature Embedding for Malware Detection

Feature embedding techniques have been widely used in many applications, such as face and speech recognition because they can be purposely designed for a specific function and to capture the critical semantic information which may appear at any position of an image (or sentence). Based on this concept, [4, 11, 27, 29, 38, 46] adopted it into malware detection. Though it has proven that the embedded N-grams of opcodes [18] and graph embedding [11, 46, 50] can efficiently capture unique malicious components, however, conducting the opcodes and graph embedding is time-consuming and their generalizability limited (e.g., the graph embedding tends only work well in learning the static features). Using these techniques, a unique behavior presented in a malware family that is critical to capture the variant of that malware family often tends to be regarded as noises while only common known

behaviors of malware families are captured by the CNN model, for example, the work by Microsoft collaborated with Intel demonstrates the setting of the practical value of the image-based transfer learning approach for static malware classification [4]. To address this problem, Sun et al [38] proposed a model which learns the unique information specific to a malicious code. However, it did not achieve a competitive result when only a small number of training dataset was available. Tran et al. [40] evaluated the performance of malware detection for zero-day attack malware using the matching and prototypical network. The Matching Network uses the softmax over the cosine distance with two embedding functions and the memory caches the common pattern of malware feature representation. Although these works focus on the semantic feature embedding of malicious code, most of them are limited to working well on many training samples. These existing models tend to be effective at capturing malware samples when the common attribute of malicious code is distinct but often do not consider when there are slight differences in features of the malware as is the case of many obfuscated malware variants.

3 Preliminary

Table 1 illustrates the notations we use throughout this paper.

Table 1: Notations

Notation	Description
x_i	the malware image feature of i th samples
y_t^i	the class t of i th samples
e_y	the average entropy feature of a malware family
θ_t	feature layers' parameters
W^i	i -th feature layer in \mathcal{F} 's weights
W_{sr}^i	the shared parameters for all malware families
W_{ts}^i	the task-specific parameters for each family
c_i	the center point of each class
L_e	the embedding loss
$L_{b,c}$	binary cross entropy loss with center loss
d_w^i	the distance feature of a pairs of images
y_d	the label of pairs of images
F_w	the convolutional filter with parameters w
β	the hyper-parameters

3.1 Control Flow Obfuscation

Malware obfuscation is a technique that is applied by malware authors to create new malware variants to avoid detection without creating a completely brand new malware signature. Among many different obfuscation techniques, we focus on control flow obfuscation which involves creating a new malware variant by reordering the control flow of functional logic from the original malware program [6]. This type of obfuscation technique makes the compiled malicious code appear to be different from the existing malware signature thus can easily avoid detection. There are three different types of control flow obfuscation our model can detect.

Function Logic Shuffling

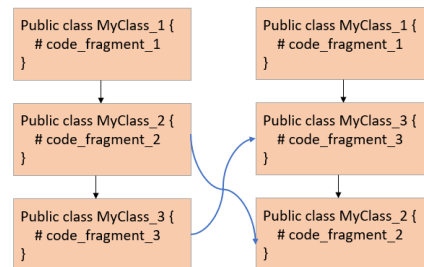


Fig. 1: Function Logic Shuffling

This technique alters the control flow path of a malware program by shuffling the order of function calls without affecting the semantics (i.e., purpose) of the original malware program. Though the functionality between the original malware and obfuscated version stays the same, because of the change of appearance in the compiled code, they appear to be different malware families, when in fact, they belong to the same malware family. An example is shown in Fig. 1 where the order of function logic MyClass_2 and MyClass_3 is changed.

Junk Code Insertion

In this technique, the malware author inserts many (junk) code that never gets executed, either after unconditional jumps, calls that never return, or conditional jumps with conditions that would never be met. The main goal of this technique is to change the control flow path to avoid detection

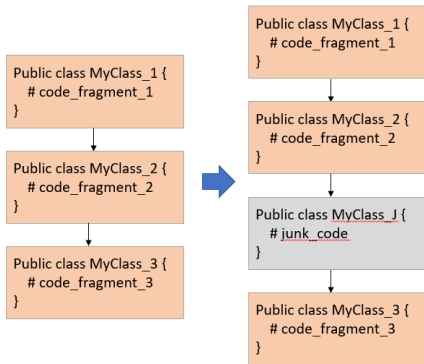


Fig. 2: Junk Code Insertion

or to waste the time for the reverse engineer analyzing useless code. An example of a junk code insertion is shown in Fig. 2 where a junk code `MyClass_J` is added in between two normal function calls.

Function Splitting

With this technique, the malware author applies the function splitting method where a function code is fragmented into several pieces each of which piece is inserted across the control flow. This technique splits the function into n code fragments or merging pieces of unrelated codes to make the changes in the compiled code. An example of a function splitting is shown Fig. 3 where two splits from `MyClass_2` are generated and randomly added among other function calls.

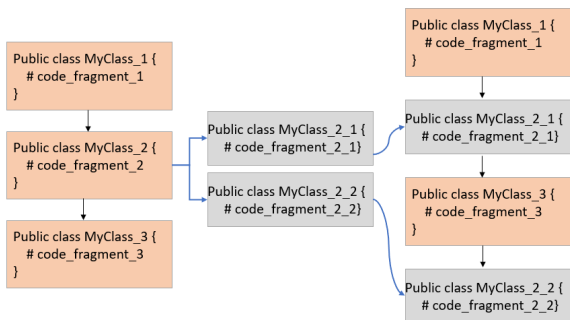


Fig. 3: Function Splitting

Though the functionality between the original malware and obfuscated versions (e.g., malware variants) stays the same, a malware code applied with the control flow obfuscation can easily avoid detection from many anti-virus programs [6]. To

address this, we propose a model resilient against the presence of many variants of malware created as a result of applying the control flow obfuscation technique. Our proposed method utilizes the information gain calculated through the entropy features associated with each malware variant. In our proposal, the entropy features measure the amount of uncertainty of a given probability distribution of a malware program that is not affected by the order of functional logic of the malware program.

3.2 Generic Approach and Issues

In the last few years, a few-shot learning technology, such as Siamese Neural Network (SNN), which uses only a few training samples to get better predictions has emerged. SNN contains two identical subnetworks (usually Convolutional Neural networks) hence the name Siamese. The two CNNs have the same configuration with the same weights, $\mathbf{W} \in \mathbf{R}^d$, where \mathbf{W} depicts the model's parameters while \mathbf{R}^d depicts the distance feature in a low dimensional space. The updating of the hyperparameters is mirrored across both CNNs which is used to find the similarity of the inputs by comparing its feature vectors.

Each parallel CNN is designed to produce an embedding (i.e., reduced dimensional representation) of the input. These embeddings can then be used to optimize a loss function during the training phase and to generate a similarity score during the testing phase.

This architecture is effectively different from traditional neural networks that learn to predict multiple classes from a large volume of datasets. This however poses a problem because they need to be retrained and updated on the whole dataset when a new class is added and removed to the dataset. SNN, on the other hand, learns a similarity function by training it to test if the two images are the same. This new architecture enables it to classify new classes of data without training the network again. This allows SNN to be more robust to class imbalance as a few images per class is sufficient for SNN to recognize those images in the future.

Fig. 4 illustrates the working of a generic SNN. The goal of the above SNN is to determine if two image samples belong to the same class or not. This is achieved through the use of two parallel

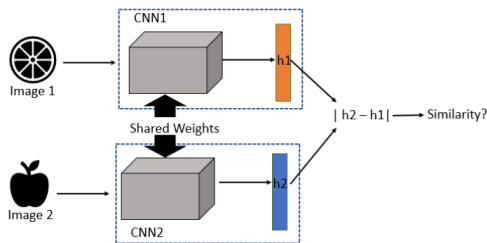


Fig. 4: The overview of Siamese Neural Network

CNNs (CNN1 and CNN2 in the above figure) trained on the two image samples (image1 and image 2 in the above figure). Each image is fed through one branch of the SNN which generates a d -dimensional feature embedding (h_1 and h_2 in the above figure) for the image. It is these feature embeddings that are used to optimize a loss function rather than the images themselves. A supervised cross-entropy function is used in SNN for the binary classification to determine whether two images are similar or dissimilar by computing $|h_2 - h_1|$ and processing it by a sigmoid function.

Mathematically, the similarity between a pair of images (x_1, x_2) within Euclidean Distance (ED) is computed in SNN using the Equation:

$$d_w(x_1, x_2) = \|F_w(x_1) - F_w(x_2)\|_2 \quad (1)$$

where the F_w indicates the feature representation for the inputted feature matrix. Generally, the model $g_w: \mathbf{R}^n$ to \mathbf{R}^d is parameterized by the weights w and its loss function is calculated using the Equation:

$$L_b = -\frac{1}{N} \sum_{i=1}^N [y_d^i f_p(d_w^{(i)}) + (1 - y_d^i) f_q(d_w^{(i)})] \quad (2)$$

where y_d denotes the label of image pairs. d_w represents the Euclidean Distance (ED) between two images at the i -th pair. Note that the most similar images are supposed to be the closest in the feature embedding space.

Though this approach would work well for finding similarities/dissimilarities across distinct image objects, this would work not well for obfuscated malware samples.

Recall that an obfuscated malware, say x_1 , changes some part of the original malware code, x_2 . When these two are converted as feature

representation, say $F_w(x_1)$ and $F_w(x_2)$, the feature values in the feature representation would look very different – this is how obfuscated malware avoids detection by anti-virus software. Inadvertently, the different values in the feature representation make the distance across obfuscated malware images very different from one another (i.e., $d_w(x_1, x_2)$ is large). Eventually, when a similarity score is computed and compared, using the loss (i.e., L_b) based on the distance calculation (i.e., $d_w(x_1, x_2)$), they would appear to be different malware families, though, in fact, they all belong to the same malware family.

4 Task-Aware Meta Learning-based Siamese Neural Network

We introduce our task-aware meta learning-based SNN model that provides a novel feature embedding better suited for control flow obfuscated malware classification. We start with the overview of our proposed model, the details of the CNN architecture that is used by our model, followed by how task-specific weights are calculated using factorization. Finally, we discuss the details of the loss functions our model use to address the challenges with the weight generation with the limited number of training samples.

4.1 Our Model

As shown in Fig. 5, our model utilizes a pre-trained network and two identical CNN networks. We use a pre-trained network (VGG-16) to compute more accurate weights for entropy features. Similarly, each CNN takes image features to calculator weight for image features and to generate a feature embedding using the task-specific weights and shared weights of both entropy and image features. The feature embeddings produced by two CNNs are used by the SNN to calculate the similarity score across intra-class variants using a new hybrid loss function.

Within each CNN, there are two sub-networks: a task-aware meta learner network and an image network - as shown in Fig. 6. The task-aware meta learner network starts by taking a task specification (e.g., entropy feature vector) and

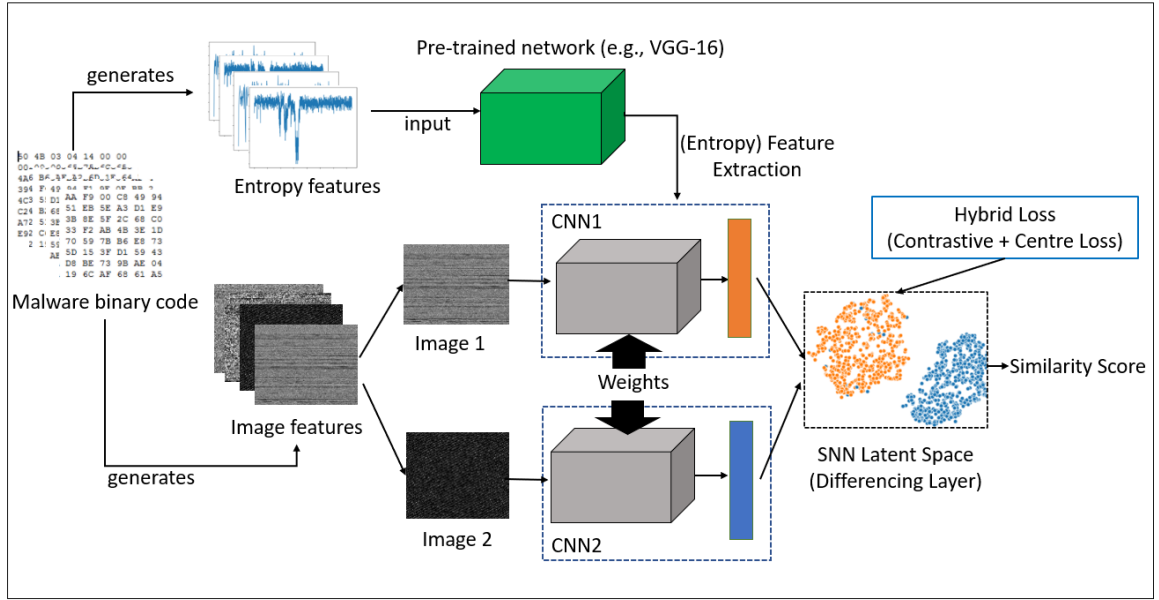


Fig. 5: Overview of our proposed model

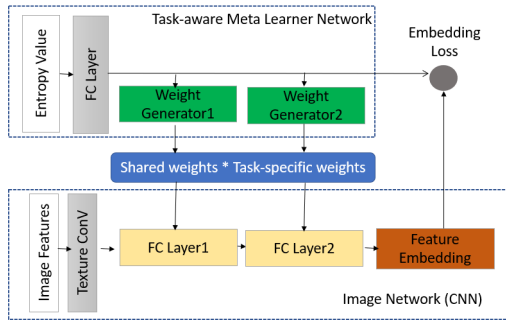


Fig. 6: CNN Architecture of our proposed model

generates the weights. At the same time, the image network (e.g., this is a typical CNN branch of a SNN) starts by taking the image feature and convoluting it until a fully connected layer is produced. The last fully connected layers use the weights generated by the task-aware meta learner network along with the shared weights to produce a task-aware feature embedding space. Embedding loss for inter-class variance is calculated for back-propagation until CNN is fully trained for all input images.

Mathematically, it can be written as the following Equation:

$$\mathbf{y} = \mathcal{F}(\mathbf{x}; \theta = \{\mathcal{G}(t), \theta_f\}) \quad (3)$$

where the SNN \mathcal{F} takes malware images \mathbf{x} as inputs and produce a task-aware feature embedding that is used by the SNN to predict the similarity $\mathbf{y} \in \{1, 0\}$ between an image pair inputted to two CNNs. Each CNN is parameterized by the weights θ which is composed of generated parameters from $\mathcal{G}(t) \in \mathcal{T}(e_y)$ and the share parameters θ_f in the $\mathcal{G}(t)$ that is shared across all malware families. The task-aware meta learner network $\mathcal{T}(e_y)$ creates a set of weight generators $g^i, i = \{1 \dots k\}$ to generate parameters for k feature layers in \mathcal{F} conditioned on θ . The overall approach of our proposed model can also be summarised using the following Algorithm 1.

4.2 Task-aware Meta Learner

Our task-aware meta learner provides two important functionalities. One is generating optimized task-specific weights using the entropy values extracted from a pre-trained deep learning model (e.g., VGG-16). Another function it provides is to work with the image network to compute the new weights based on the shared weights and the task-specific weights so that the embedding loss is accurately calculated to capture the relative distance across inter-class variance (e.g., the features of the image). These functions are necessary since some malware samples (e.g.,

zero-day attack samples) usually are much smaller than the number of images required for training a SNN model

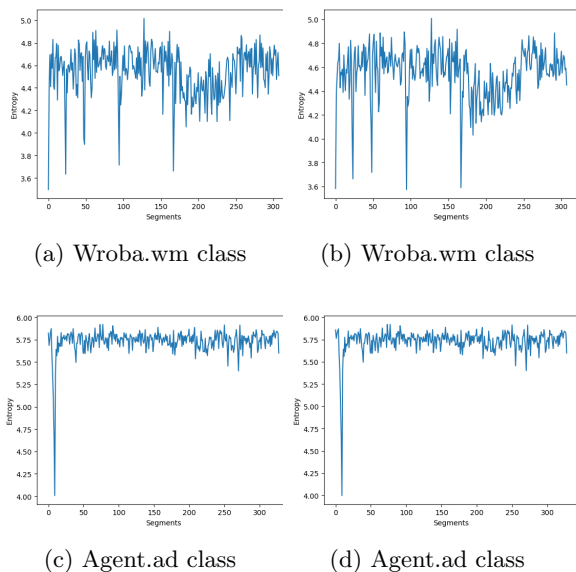


Fig. 7: Examples of entropy graphs of two malware families

Using the entropy values, our meta learner recognizes a specific malware signature present in the entropy so that later it uses this knowledge to find whether some malware samples are derived from the same malware family or not (e.g., obfuscated malware). The entropy values are extracted from the VGG-16 when entropy graphs are inputted.

We use entropy graphs to recognize a unique malware signature belonging to each malware family. To illustrate the use of an entropy graph as a task specification, we show four samples of malware images as shown in Fig.7. Fig.7 (a) and Fig.7 (b) are two obfuscated malware samples from the same Wroba.wm family. Similarly, Fig.7 (c) and Fig.7 (d) of the name Agent.ad are from the same Agent family. One can see that the entropy graphs within the same family share a similar pattern while there are visible differences in the entropy graphs between two different malware families.

Our task-aware meta learner utilizes the entropy values extracted from the entropy graph

to train our proposed model to recognize if an image pair is similar or dissimilar (i.e., belong to the same malware family or not) – see Algorithm 10. To obtain an entropy graph, a malware binary file is read as a stream of bytes and separated into a few segments. The frequency of unique byte value is counted and computes the entropy using Shannon’s formula as follows:

$$Ent = - \sum_i \sum_j M(i, j) \log M(i, j) \quad (4)$$

where M is the probability of an occurrence of a byte value. The entropy obtains the minimum value of 0 when all the byte values in a binary file are the same while the maximum entropy value of 8 is obtained when all the byte values are different. The entropy values are then represented as a stream of values which can be reshaped as an entropy graph. The entropy graph is then converted as a feature vector inputted through the convolutional extractor of a pre-trained network (e.g., VGG-16 [32]). The summary of the steps involved in the entropy graph is described in Algorithm 2.

Algorithm 1 Pseudo-code of our proposed algorithm

```

1: procedure UNSEEN TEST(Query Test)
2:   Initialization : network parameters
3:   Sample batch of tasks  $\{\mathcal{G}(t) \sim \mathcal{F}(\tau) : \text{gray}$ 
   scale feature  $(x_i, y_i)$ , family entropy data  $e_y$ ,
   pair data  $(d_w, y_d)$ 
4:   for n=1 to  $N$  do do
5:      $W_{ts}^i \leftarrow$  branch of meta learner  $\tau(e_y)$ 
6:      $W_{sr}^i \leftarrow$  branch of SNN  $\mathcal{F}(x_i)$ 
7:      $W^i \leftarrow W_{sr}^i \cdot \text{diag}(W_{ts}^i)$ 
8:      $d^i \leftarrow \{\text{branch}(W^i) - \text{branch}(W^j)\}$ 
9:      $d_w^i \leftarrow \text{centerlayer}(d^i)$ 
10:    update  $\theta \leftarrow L_e(W^i) + L_{bc}(d_w^i)$ 
11:   end for
12: end procedure

```

4.3 Weight Generator via Factorization

In the generic SNN approach, the feature extractor only uses the image feature. This approach however is no longer effective in

Algorithm 2 Pseudo-code of entropy graph

```

1: procedure ENTROPY GRAPH
2:    $f$ : malware binary file;  $l$ : segment length;
    $n$ : the number of files
3:   while not reach to  $n$  do
4:     read  $l$  bytes from  $f$ , and defined as
     segment  $s$ ;
5:     for  $i = 0$  to 255 do
6:       computing the probability  $p_i$  of  $i$ 
       appearing in  $s$ ;
7:       computing the Shannon entropy
8:     end for
9:   end while
10: end procedure

```

the detection of obfuscated malware where multiple obfuscated malware samples contain almost identical image features.

The problem is further complicated when only a few samples (i.e., less than 5 malware samples) exist (i.e., not enough malware feature information to use for classification as there are very small variations of malware samples to be collected from a small number of malware samples). To address this issue, we present a new novel weight generation scheme based on the work presented by [10]. In our proposed model, the weight generator $G(\cdot, \cdot | \phi)$ gets as input the entropy vectors W_{ave} of a class in addition to the image vectors $\mathbf{Z}' = \{z'_i\}_{i=1}^N$ of the N training samples of the corresponding class. This results a weight vector $w' = G(\mathbf{Z}', W_{ave})$.

In our model, the weight generator scheme is incorporated in the Fully-Connected (FC) layer to solve the non-linear issue that exists in the relationship between the entropy feature and malware image. By integrating the weight generator at the FC layer, the weights of the features extracted before the FC layers can be integrated better into calculating new and more optimized weights for the whole model. We generate weights by creating a weight combination. The weight combination produces the composite features that encode the non-linear connection in the feature space. This is done by multiplying the entropy features and image features together such that the composite features learn a feature embedding resistance to different obfuscated malware variations. Note that the dimension of the weight generator g^i on the FC

layer must be matched with the dimension of the weight size of the i th feature layers in F , so that the weights $W_i \in \mathbf{R}^{m \times n}$ can be decomposed using the following Equation:

$$W^i = W_{sr}^i \cdot \text{diag}(W_{ts}^i) \quad (5)$$

where $W_{sr}^i \in \mathbf{R}^{m \times n}$ is the shared parameters for all malware family $\{t_1, \dots, t_N\}$ and $W_{ts}^i \in \mathbf{R}^n$ is the task-specific parameter for each malware family. With such factorization, the weight generators only need to generate the malware-specific parameters for each malware family in the lower dimension and learn one set of parameters in the high dimension shared across all malware families.

4.4 Loss Function

Our proposed model uses two different types of loss functions. Embedding loss is used by our task-aware meta learner network to compute a loss across the inter-class variance (e.g., the features in the feature embedding space of a CNN branch) while a hybrid loss is used by the differencing layer of the SNN to compute the similarities across inter-class variants between an image pair.

4.4.1 Embedding Loss for Meta Learner

The feature representation of the entropy graph of a malware class can be easily influenced by binary loss. This is because the use of binary loss can only give the probability of the distribution of distances between positive and negative image pairs. It cannot estimate the probabilities of distances between positive and negative image pairs across different malware variations therefore not being able to correctly classify similar pairs of images across obfuscated malware samples (i.e., cannot learn a discriminative feature during the training procedure). To address this issue, we add a secondary cross-entropy loss not only to learn the discriminative feature but also the effect of overfitting caused by contrastive loss. This embedding loss is defined using the following Equation.

$$L_e = -\frac{1}{N} \sum_{i=1}^N \sum_{t=1}^T \log \left[\frac{\exp(F(x_i; \theta_t)) \cdot y_t^i}{\sum_{j=1}^T \exp(F(x_i; \theta_t))} \right] \quad (6)$$

where x^i represents the i th sample in the dataset of the size N . $y_t \in \{0, 1\}^t$ indicates the one-hot encoding applied to the input based on the labels. T indicates the number of tasks during training (e.g., either in the whole dataset or in the minibatch).

4.4.2 Hybrid Loss for Our SNN

To calculate the similarity score for our proposed model, we propose a hybrid loss function comprised of a center loss and a contractive loss. The center loss proposed by Wen et. al. [44] was a supplement loss function to the softmax loss for the classification task. It can learn to find a sample that can act as the center image of each class and try to shorten the distance across the training samples of similar features by moving them to be closer to the center of the sample as much as possible. This center loss can be calculated as follows:

$$L_c = \frac{1}{2N} \sum_N^{i=1} \left\| d_w^{(i)} - c_i \right\|_2^2 \quad (7)$$

where c_i denotes the center of class i while $d_w^{(i)}$ denoting the features of the euclidean distance. The objective function stands for the squared Euclidean distance. Intuitively, the center loss encourages instances of the same classes to be closer to a learned class center.

However, this approach doesn't address the issue of moving apart from the training samples of dissimilar features. To address this issue, we propose the hybrid loss function integrated with the pairwise center to better project the latent task embedding $e_t = T(t)$ into a joint embedding space that contains both the negative and positive center points.

We adopt a metric learning approach where the corresponding learned feature is closer to the joint feature embedding for positive inputs of a given image pair while the corresponding learned feature is far away from the joint feature embedding for negative inputs of a given image pair.

$$\min L = \beta \min L_e + L_{b,c} \quad (8)$$

where β is the hyperparameter to balance the two terms. In our study, we set it at 0.8.

Our experimental results, shown in Fig.11, illustrate that the β value at 0.8 provides the best

performance when it was tested on one-shot N-way learning. This result also confirms that the hybrid multi-loss function can reduce the distance between the same classes and enlarge the distance between the different classes. Additionally, it does not change the attribute of the feature in the feature space, so the optimization of this layer will never negatively affect the deeper network layers. This hybrid loss function can also compute classification accuracy with a learned distance threshold on distances.

5 Experiments

In this section, we describe the details of datasets we used for experiments, model configuration, and the results of our experiments. The results were obtained by running the experiments on the desktop with the 32GM RAM, Nvidia Geforce RTX 2070(8GB), and Intel(R) Core(TM) i7-9700 CPU @ 3.00 GHz.

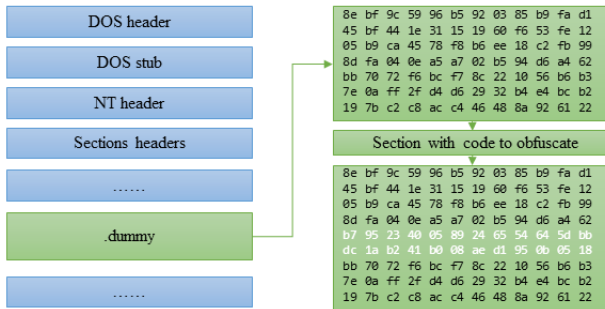
5.1 Andro-dumpsys Dataset

We use the Andro-dumpsys dataset obtained from [14] that has been widely used for malware detection. The original dataset consists of 906 malicious binary files from 13 malware families. As illustrated in Table 2, the number of the malware variants and the total number of samples from different malware families varied. Almost half of the malware family had no more than 25 malware samples while some only had one sample as they were most likely the new malware detected lately (e.g., Blocal and Newbak). In addition to the original dataset, we also generated three additional synthetic malware variants each of which is applied with different control flow obfuscation techniques described earlier: function logic shuffling, junk code insertion, and function splitting, respectively. Two samples from each additional malware variant, a total of 6 additional samples, for each malware family were added to the original dataset.

Fig. 8 illustrates a snippet of how obfuscated malware is created by applying a junk code insertion. In this example, we created a dummy array that acts as a junk code and added in between two function calls from the original malware code. We applied a similar approach for the other two types of control flow obfuscation.

Table 2: Andro-dumpy Dataset.

No.	Family	Vvariants (+3 Synthetic)	Samples (+ 6 Synthetic)
1	Agent	39 (42)	150 (156)
2	Blocal	1 (4)	1 (7)
3	Climap	1 (4)	5 (11)
4	Fakeguard	1 (4)	10 (16)
5	Fech	1 (4)	3 (9)
6	Gepew	4 (7)	112 (118)
7	Gidix	6 (9)	108 (114)
8	Helir	1 (4)	15 (21)
9	Newbak	1 (4)	1 (7)
10	Recal	2 (5)	25 (31)
11	SmForw	23 (26)	166 (172)
12	Tebak	10 (13)	93 (99)
13	Wroba	23 (26)	108 (114)

**Fig. 8:** Example of Inserting Junk code

We also increased the image sample size to have at least 30 samples for every malware family using a data argumentation technique (e.g., applying random transformations such as image rotations, re-scaling, and clipping the images horizontally). The details of the argumentation parameters are as shown in Table 3.

Table 3: Data augmentation parameters

Methods	Values	Description
rescale	1./255	Resizing an image by a given scaling factor.
zca_epsilon	1e-06	Epsilon for ZCA whitening
fill_mode	wrap	Points outside the boundaries of the input are filled according to the mode
rotation_range	0.1	Setting degree of range for random rotations.
height_shift_range	0.5	Setting range for random vertical shifts
horizontal_flip	True	Randomly flips inputs horizontally

5.1.1 Image Feature

We use the same technique proposed by [49] to produce image features. To produce image features, we first read the binary malware as a vector of 8-bit unsigned integers which are then converted into 2D vectors. We use the fixed width while the height is decided according to the size of the original file. Finally, the 2D vector is converted into the gray images using the color range [0, 255]. Note that the gray images at this stage are different dimensions according to the varying heights and widths in size which biases could occur in the fully connected layer. To address this issue, we use the bilinear interpolation method, as suggested by [21], to produce our image feature in uniform to the size of 105×105 .

5.1.2 Entropy Feature

To obtain the entropy feature of each malware family, we take each byte of the malware binary file as a random variable and count the frequency of each value (00h-FFh). More concretely, the byte reads from the binary file are divided into several segments. For each segment, we first calculate the frequency of each byte value $p_j (1 \leq j \leq m)$ and secondly the entropy y_i of the segment is calculated. The entropy values are then represented as a stream of values which can be reshaped as an entropy graph with the size of $254 \times 254 \times 1$. These entropy graphs are then converted as a 4096-dimensional feature vector inputted through the convolutional extractor of the VGG-16 architecture [32].

5.2 Model Configurations

The task-aware meta learner network $\mathcal{T}(t)$ is a two-layer FC network with a hidden unit size of 512 except for the top layer which is 4096 for input. The weight generator g^i is a single FC layer with the output dimension the same as the output dimension of the corresponding feature layer in \mathcal{F} . We add a Relu function to the output of g^i . In the case where the processed malware images are used as inputs, and the convolutional part is configured as the 4-layer convolutional network (excluding pooling layers) following the structure as [16]. Besides, the Relu function and batch normalization are added after by the convolution layer and FC layer. The total number

of parameters in our proposed model is 40 million. The overview of our network configurations is described in Fig. 9.

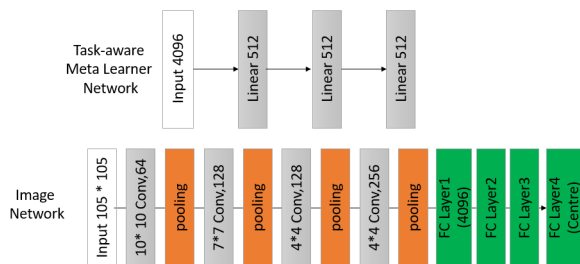


Fig. 9: Network Configurations

5.3 Results

We set the batch size to 32 and used Adam as the optimizer with the initial learning rate of 10^{-4} for the image network and the weight generators, and 10^{-5} for the task embedding network. The network is trained with 100 epochs, which ran for approximately 1.5 hours. As Fig. 11 illustrates, both train and validation loss stabilizes after 50 epochs confirming the training is done by this stage.

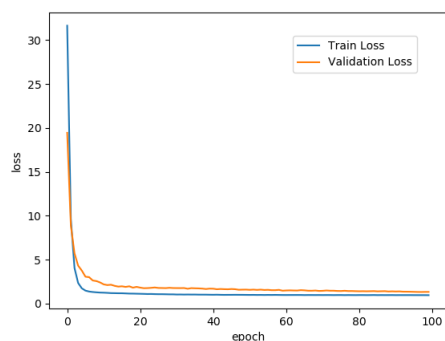


Fig. 10: Loss during Training on Epochs

The testing process conducts M times of N -way on N -shot learning tasks, where Q times of correct predictions contribute to the accuracy calculated by the following formula:

$$Accuracy = (100 * Q/m)\% \quad (9)$$

5.3.1 N-way matching accuracy

The evaluation of N -way learning at each test state is carried out for one-shot and 5-shot. For N -way one-shot learning, we choose an anchor image from one class of test, and then randomly selects N classes of images to form the support set $X = \{x_i\}_{i=1}^N$, where $x_1, \forall x \in X$, where selected image's class is the same as the anchor image \hat{x} , the other images in support sets are from different classes. The similarity score between \hat{x} and other images is calculated through our model. To be specific, if the similarity score of the feature vector of x_1 , which can be represented as $S = \{s_i\}_{i=1}^N$, that score is the maximum of S the task can be labeled as a correct prediction. Otherwise, it is regarded as an incorrect prediction. For N -way 5-shot learning, we randomly select N unseen classes and six instances, in which five instances of each class are randomly selected as the support set, $X = \{x_1, \dots, x_i\}_{i=5}^N$ and the remaining instances of each class form the query set. Its prediction procedure is the same as the test in the one-shot.

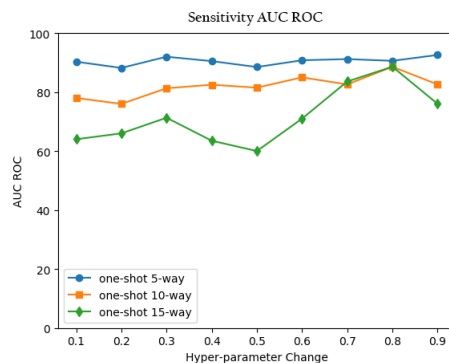
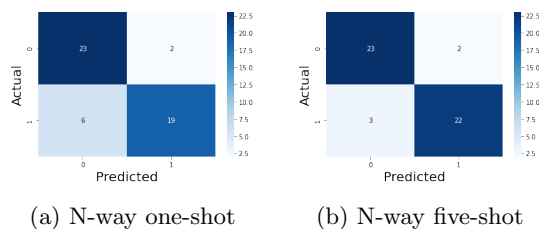


Fig. 11: One-shot N-way Convergence

The matching accuracies of N -way accuracy for the one-shot and 5-shot are illustrated in Fig.12. We randomly used 50 pairs of images, 25 containing positive image pairs and 25 containing negative image pairs, to test the effectiveness of our proposed model. As shown in the N -way one-shot result in Fig.12 (a), 19 out of 25 positive image pairs were matched correctly where there were 6 true negatives (i.e., 2 positive pairs not matched correctly). Similarly, 23 of 25

**Fig. 12:** Matching Accuracy

negative pairs matched correctly while there were 2 false positives (i.e., 2 negative pairs matched incorrectly). For the N-way 5-shot results (shown in Fig.12 (b)), the accuracy of matching is higher as almost 22 out 25 pairs matched correctly for both positive and negative pairs, there were 3 incorrectly matched results.

5.3.2 Embedding space projection

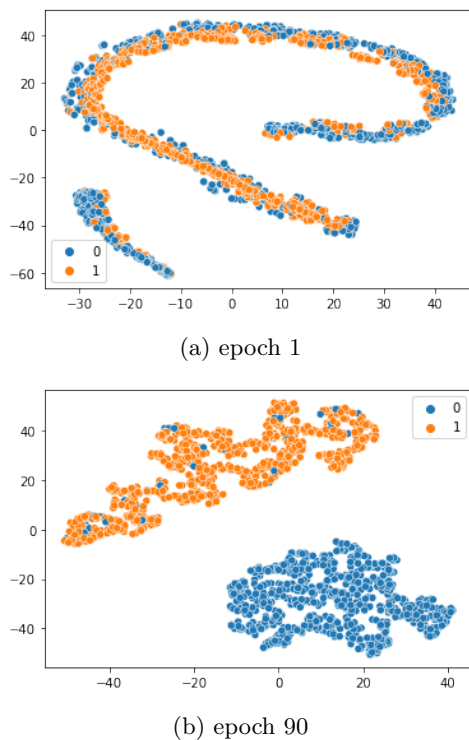
**Fig. 13:** Feature Embedding Before vs. After Training

Fig.13 shows the projection of the embeddings space using the 2- dimensional Principal

Component Analysis (PCA) technique, where each orange point dictates the distance of a positive pair while each blue point dictates the distance of a negative pair. Fig.13 (a) is the embedding space before training while Fig.13 (b) projects the embedding space after training. After training, we can clearly see two distinct clusters - one around the distance calculated for all positive pairs and the other for negative pairs. This confirms that our proposed model has learned well to distinguish the similarities among positive pairs and negative pairs and separate them far apart.

Table 4: Comparison of classification performance of different few-shot learning approaches for Andro-dumpy datasets

1-shot				
Ref.	Method	5-way	10-way	15-way
[42]	Matching Network	83.5	82.1	74.9
[34]	Prototypical Network	85.4	80.7	79.3
[16]	Siamese Network	80.2	67.7	63.5
	Task-aware SNN	88.1	86.6	82.1
5-shot				
Ref.	Method	5-way	10-way	15-way
[42]	Matching Network	88.6	84.1	76.2
[34]	Prototypical Network	83.8	80.8	79.5
[16]	Siamese Network	83.4	71.5	68.7
	Task-aware SNN	91.2	88.5	83.5

5.3.3 Benchmark against similar methods

Table. 4 shows the result of benchmarking our proposed model against the current state-of-the-art, especially along with the Matching network and Prototypical network, as well as the original Siamese Network. Our model surpassed the performance of the Matching Network and Prototypical Network by 4.6% and 2.7% on the 1-shot learning on the 5-way. The difference between our results of 1-shot and 5-shot was 3.1%, 1.9%, 1.4% on the 5-way, 10-way, 15-way respectively. Our proposed 5-shot result outperformed all three exiting models by 2.6%, 7.4%, 7.8% respectively on the 5-way.

5.3.4 Distance measure effectiveness

We also examine the effectiveness of our proposed model in distance measurement by using the AUC (Area Under The Curve) ROC (Receiver Operating Characteristics) curve. The AUC-ROC curve is commonly composed of two performance measures, true-positive (FPR) rate and false-positive rate (FPR) rate, respectively. The equations related to these two performance measures of the ROC curve are shown as follows:

$$\begin{aligned} FPR(P^*) &:= \int_{P^*}^1 f_0(p) dp \\ TPR(P^*) &:= \int_{P^*}^1 f_1(p) dp \end{aligned} \quad (10)$$

where the $f_0(p)$ is denoted by the probability of a density function for the predictions $p(x)$ produced by our proposed model. The negative pairs are labeled as 0, and $f_1(p)$ is the probability from the positive pair that is labeled as 1. The given discrimination threshold P are the integrals of the tails of these distributions according to the true-positive rate and false-positive rate. Based on the two parameters TPR and FPR, the AUC-ROC curve is defined as follows:

$$AUC - ROC = \int_0^1 TPR(FPR)D(FPR) \quad (11)$$

where the AUC measures the entire two-dimensional area underneath the entire ROC curve (i.e., integral calculus) from (0,0) to (1,1). For example, a model whose predictions are 100% wrong has an AUC of 0.0 while a model whose predictions are 100% correct has an AUC of 1.0. Using this concept, we demonstrate the result predicted by the saved weights of 1 shot and 5-shot respectively of the learned model on the test set including 5-way, 10-way, and 15-way. These AUC-ROC curves are shown in Fig 14. As it shows, our result is on a set of points in the true positive rate - false positive rate plane. The results achieve the AUC-ROC equals 0.92, 0.91, and 0.80 respectively under the 5-way, 10-way, and 15-way on the one-shot learning. We further conducted the AUC-ROC on the 5-shot learning. Our proposed model also obtained better performance than the generic SNN with

95.6%, 90.7%, 86.8% at 5-way, 10-way, and 15-way respectively. As expected, the accuracy of both 1-shot and 5-shot drops as the number of N-way increases with higher intra-class variance.

Note that our model always performs better as shown in these graphs as the AUC-ROC areas (i.e., the areas up to the blue line) of our proposed is larger compared to the generic SNN.

6 Conclusion

We proposed a novel task-aware meta learning-based Siamese Neural Network to accurately classify different malware families even in the presence of obfuscated malware variants. Each branch of CNN used by our model has an additional network called “task-aware meta learner network” that can generate task-specific weights using the entropy graphs obtained from malware binary code. By combining the weigh specific parameters with the shared parameters, each CNN in our proposed model produces the fully connected feature layers so that the feature embedding at each CNN is accurately adjusted for different malware families despite there are obfuscated malware variants in each malware family.

In addition, our proposed model can provide accurate similarity scores even if it is trained with a limited number of samples. Our model also uses a pre-trained VGG-16 network in a meta-learning fashion to computer accurate weight factors for entropy features. This meta-learning approach essential solves the issues that are associated with creating potential bias due to not having enough training samples.

Our model also offers two different types of innovative loss functions that can more accurately compute the similarity scores within a CNN and the feature embeddings used by two CNNs.

Our experimental results show that our proposed model is highly effective in recognizing the presence of unique malware signatures thus able to correctly classify obfuscated malware variants that belong to the same malware family.

We are planning to apply different types of malware samples (e.g., DDoS attack [43] and ransomware families [22, 23, 51, 52]) and other data samples (e.g., finding similar abnormalities in medical x-ray images [7]) to test the generalizability of our model.

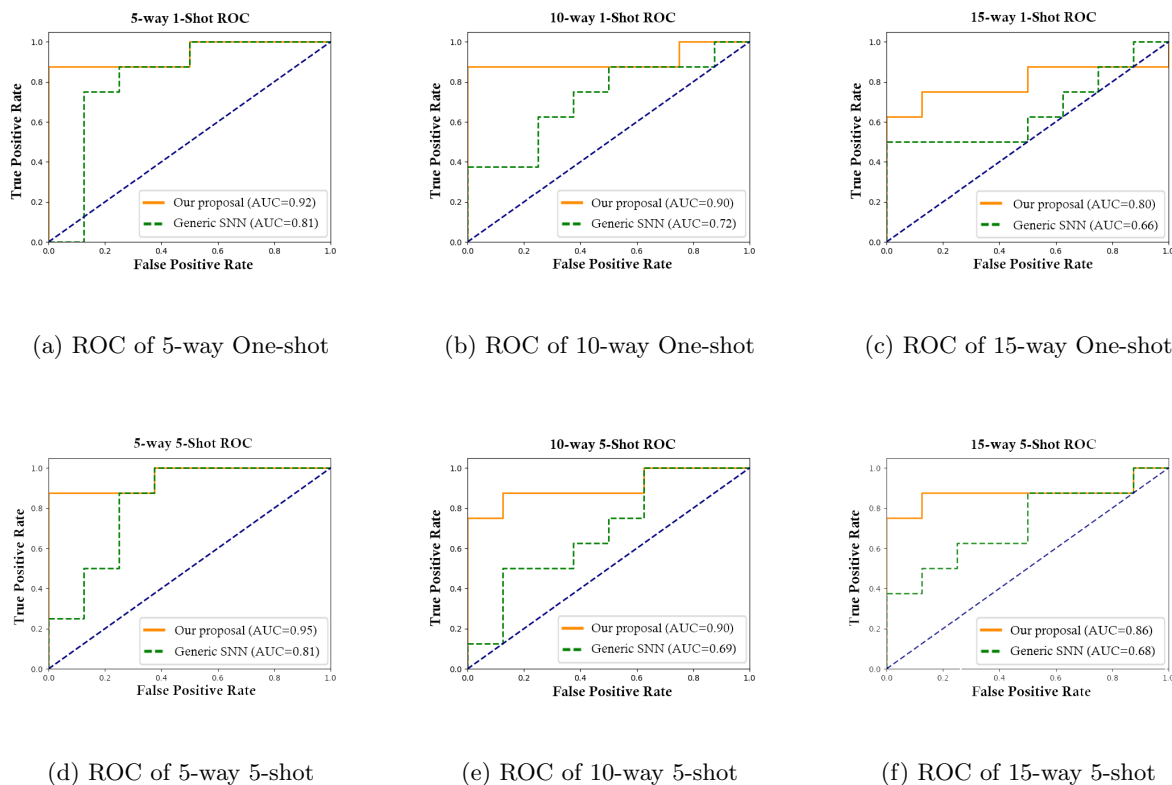


Fig. 14: AUC-ROC curves under the N-way N-shot

Acknowledgment

This research is supported by the Cyber Security Research Programme—Artificial Intelligence for Automating Response to Threats from the Ministry of Business, Innovation, and Employment (MBIE) of New Zealand as a part of the Catalyst Strategy Funds under the grant number MAUX1912.

References

- [1] Akarsh S, Poornachandran P, Menon VK, et al (2019) A detailed investigation and analysis of deep learning architectures and visualization techniques for malware family identification. In: *Cybersecurity and Secure Information Systems*. Springer, p 241–286
- [2] Bacci A, Bartoli A, Martinelli F, et al (2018) Detection of obfuscation techniques in android applications. In: *Proceedings of the 13th International Conference on Availability, Reliability and Security*, pp 1–9
- [3] Cao J, Su Z, Yu L, et al (2018) Softmax cross entropy loss with unbiased decision boundary for image classification. In: *2018 Chinese Automation Congress (CAC)*, IEEE, pp 2028–2032
- [4] Chen L, Sahita R, Parikh J, et al (2020) Stamina: Scalable deep learning approach for malware classification. Intel Labs Whitepaper, <https://www.intel.com/content/www/us/en/artificial-intelligence/documents/stamina-deep-learning-for-malware-protection-whitepaper.html>

- [5] Chua M, Balachandran V (2018) Effectiveness of android obfuscation on evading anti-malware. In: Proceedings of the Eighth ACM Conference on Data and Application Security and Privacy, pp 143–145
- [6] Dong S, Li M, Diao W, et al (2018) Understanding android obfuscation techniques: A large-scale investigation in the wild. In: International Conference on Security and Privacy in Communication Systems, Springer, pp 172–192
- [7] Feng S, Liu Q, Patel A, et al (2022) Automated pneumothorax triaging in chest x-rays in the new zealand population using deep-learning algorithms. *Journal of Medical Imaging and Radiation Oncology*
- [8] Gibert D, Mateu C, Planes J, et al (2018) Classification of malware by using structural entropy on convolutional neural networks. In: Proceedings of the AAAI Conference on Artificial Intelligence
- [9] Gibert D, Mateu C, Planes J (2019) A hierarchical convolutional neural network for malware classification. In: 2019 International Joint Conference on Neural Networks (IJCNN), IEEE, pp 1–8
- [10] Gidaris S, Komodakis N (2018) Dynamic few-shot visual learning without forgetting. In: Proceedings of the IEEE Conference on Computer Vision and Pattern Recognition, pp 4367–4375
- [11] Hashemi H, Azmoodeh A, Hamzeh A, et al (2017) Graph embedding as a new approach for unknown malware detection. *Journal of Computer Virology and Hacking Techniques* 13(3):153–166
- [12] Hsiao SC, Kao DY, Liu ZY, et al (2019) Malware image classification using one-shot learning with siamese networks. *Procedia Computer Science* 159:1863–1871
- [13] Hu X, Griffin KE, Bhatkar SB (2014) Encoding machine code instructions for static feature based malware clustering. US Patent 8,826,439
- [14] Jang J, Kang H, Woo J, et al (2016) Andro-dumpsys: Anti-malware system based on the similarity of malware creator and malware centric information. *Computers Security* 58:125 – 138. <https://doi.org/http://dx.doi.org/10.1016/j.cose.2015.12.005>, URL <http://www.sciencedirect.com/science/article/pii/S016740481600002X>
- [15] Kalash M, Roohan M, Mohammed N, et al (2018) Malware classification with deep convolutional neural networks. In: 2018 9th IFIP international conference on new technologies, mobility and security (NTMS), IEEE, pp 1–5
- [16] Koch G, Zemel R, Salakhutdinov R (2015) Siamese neural networks for one-shot image recognition. In: ICML deep learning workshop, Lille
- [17] Lee Y, Woo S, Lee J, et al (2019) Enhanced android app-repackaging attack on in-vehicle network. *Wireless Communications and Mobile Computing* 2019
- [18] Li X, Qiu K, Qian C, et al (2020) An adversarial machine learning method based on opcode n-grams feature in malware detection. In: 2020 IEEE Fifth International Conference on Data Science in Cyberspace (DSC), IEEE, pp 380–387
- [19] Luo JS, Lo DCT (2017) Binary malware image classification using machine learning with local binary pattern. In: 2017 IEEE International Conference on Big Data (Big Data), IEEE, pp 4664–4667
- [20] Makandar A, Patrot A (2018) Trojan malware image pattern classification. In: Proceedings of International Conference on Cognition and Recognition, Springer, pp 253–262
- [21] Malvar HS, He Lw, Cutler R (2004) High-quality linear interpolation for demosaicing of bayer-patterned color images. In: 2004 IEEE International Conference on Acoustics, Speech, and Signal Processing, IEEE, pp iii–485

- [22] McIntosh T, Jang-Jaccard J, Watters P, et al (2019) The inadequacy of entropy-based ransomware detection. In: International Conference on Neural Information Processing, Springer, pp 181–189
- [23] McIntosh TR, Jang-Jaccard J, Watters PA (2018) Large scale behavioral analysis of ransomware attacks. In: International Conference on Neural Information Processing, Springer, pp 217–229
- [24] Milosevic N, Dehghantanha A, Choo KKR (2017) Machine learning aided android malware classification. *Computers Electrical Engineering* 61:266–274
- [25] Moustakidis S, Karlsson P (2020) A novel feature extraction methodology using siamese convolutional neural networks for intrusion detection. *Cybersecurity* 3(1):1–13
- [26] Naeem H, Ullah F, Naeem MR, et al (2020) Malware detection in industrial internet of things based on hybrid image visualization and deep learning model. *Ad Hoc Networks* 105:102,154
- [27] Ng CK, Jiang F, Zhang LY, et al (2019) Static malware clustering using enhanced deep embedding method. *Concurrency and Computation: Practice and Experience* 31(19):e5234
- [28] Ni S, Qian Q, Zhang R (2018) Malware identification using visualization images and deep learning. *Computers Security* 77:871–885
- [29] Pektaş A, Acarman T (2020) Deep learning for effective android malware detection using api call graph embeddings. *Soft Computing* 24(2):1027–1043
- [30] Raff E, Zak R, Cox R, et al (2018) An investigation of byte n-gram features for malware classification. *Journal of Computer Virology and Hacking Techniques* 14(1):1–20
- [31] Shen J, Cao X, Li Y, et al (2018) Feature adaptation and augmentation for cross-scene hyperspectral image classification. *IEEE Geoscience and Remote Sensing Letters* 15(4):622–626
- [32] Simonyan K, Zisserman A (2014) Very deep convolutional networks for large-scale image recognition. arXiv preprint arXiv:14091556
- [33] Singh A, Dutta D, Saha A (2019) Migan: malware image synthesis using gans. In: Proceedings of the AAAI Conference on Artificial Intelligence, pp 10,033–10,034
- [34] Snell J, Swersky K, Zemel RS (2017) Prototypical networks for few-shot learning. arXiv preprint arXiv:170305175
- [35] Song L, Tang Z, Li Z, et al (2017) Appis: Protect android apps against runtime repackaging attacks. In: 2017 IEEE 23rd International Conference on Parallel and Distributed Systems (ICPADS), IEEE, pp 25–32
- [36] Su J, Vasconcellos DV, Prasad S, et al (2018) Lightweight classification of iot malware based on image recognition. In: 2018 IEEE 42Nd annual computer software and applications conference (COMPSAC), IEEE, pp 664–669
- [37] Sun B, Li Q, Guo Y, et al (2017) Malware family classification method based on static feature extraction. In: 2017 3rd IEEE International Conference on Computer and Communications (ICCC), IEEE, pp 507–513
- [38] Sun G, Qian Q (2018) Deep learning and visualization for identifying malware families. *IEEE Transactions on Dependable and Secure Computing*
- [39] Tang Z, Wang P, Wang J (2020) Convprotonet: Deep prototype induction towards better class representation for few-shot malware classification. *Applied Sciences* 10(8):2847
- [40] Tran TK, Sato H, Kubo M (2019) Image-based unknown malware classification with few-shot learning models. In: 2019 Seventh International Symposium on Computing and Networking Workshops (CANDARW), IEEE,

pp 401–407

- [41] Vasan D, Alazab M, Wassan S, et al (2020) Image-based malware classification using ensemble of cnn architectures (imcec). *Computers Security* p 101748
- [42] Vinyals O, Blundell C, Lillicrap T, et al (2016) Matching networks for one shot learning. *arXiv preprint arXiv:160604080*
- [43] Wei Y, Jang-Jaccard J, Sabrina F, et al (2021) Ae-mlp: A hybrid deep learning approach for ddos detection and classification. *IEEE Access* 9:146,810–146,821
- [44] Wen Y, Zhang K, Li Z, et al (2016) A discriminative feature learning approach for deep face recognition. In: *European conference on computer vision*, Springer, pp 499–515
- [45] Yuan B, Wang J, Liu D, et al (2020) Byte-level malware classification based on markov images and deep learning. *Computers Security* 92:101,740
- [46] Zhang B, Xiao W, Xiao X, et al (2020) Ransomware classification using patch-based cnn and self-attention network on embedded n-grams of opcodes. *Future Generation Computer Systems* 110:708–720
- [47] Zheng X, Pan L, Yilmaz E (2017) Security analysis of modern mission critical android mobile applications. In: *Proceedings of the Australasian Computer Science Week Multiconference*, pp 1–9
- [48] Zhu HJ, You ZH, Zhu ZX, et al (2018) Droiddet: effective and robust detection of android malware using static analysis along with rotation forest model. *Neurocomputing* 272:638–646
- [49] Zhu J, Jang-Jaccard J, Watters PA (2020) Multi-loss siamese neural network with batch normalization layer for malware detection. *IEEE Access* 8:171,542–171,550
- [50] Zhu J, Jang-Jaccard J, Liu T, et al (2021) Joint spectral clustering based on optimal graph and feature selection. *Neural Processing Letters* 53(1):257–273
- [51] Zhu J, Jang-Jaccard J, Singh A, et al (2021) Task-aware meta learning-based siamese neural network for classifying obfuscated malware. *arXiv preprint arXiv:211013409*
- [52] Zhu J, Jang-Jaccard J, Singh A, et al (2021) A few-shot meta-learning based siamese neural network using entropy features for ransomware classification. *arXiv preprint arXiv:211200668*